

# SPREAD DATA ANALYSIS OF ALUMINUM OXIDE SPLATS REINFORCED WITH CARBON NANOTUBES

S. Asadi

\* s\_asadi@pnu.ac.ir

Received: March 2014

Accepted: September 2014

Department of Mechanical Engineering, Payame Noor University (PNU), Tehran, Iran.

**Abstract:** Coating of a surface by droplet spreading plays an important role in many novel industrial processes, such as plasma spray coating, ink jet printing, nano safeguard coatings and nano self-assembling. Data analysis of nano and micro droplet spreading can be widely used to predict and optimize coating processes. In this article, we want to select the most appropriate statistical distribution for spread data of aluminum oxide splats reinforced with carbon nanotubes. For this purpose a large class of probability models including generalized exponential (GE), Burr X (BX), Weibull (W), Burr III (BIII) distributions are fitted to data. The performance of the distributions are estimated using several statistical criteria, namely, Akaike Information Criterion (AIC), Bayesian Information Criterion (BIC), Log-Likelihood (LL) and Kolmogorov-Smirnov distance. Also, the fitted plots of probability distribution function and quantile-quantile (q-q) plots are used to verify the results of different criteria. An important implication of the present study is that the GE distribution function, in contrast to other distributions, may describe more appropriately in these datasets.

**Keywords:** Aluminum oxide, Carbon nanotube, Coating, Model selection criteria, Splat, Spread data, Statistical distribution.

## 1. INTRODUCTION

Spreading of droplets on solid surfaces is important in a wide variety of applications including plasma spray coating, ink jet printing, DNA synthesis and etc [1].

Plasma spraying is one of the thermal spray processes. The process is commonly used to apply protective coatings on components to shield them from wear, corrosion, and high temperatures. Plasma coatings are built up by agglomeration of splats formed by the impact, spread, and solidification of individual particles. Splat is the smallest unit of the microstructure of plasma sprayed coatings. The properties of the coatings are largely dependent on the splat morphology and their stacking. The splat shape is dependent on material properties of the powder; impact conditions, e.g., impact velocity and temperature; and substrate conditions, e.g., substrate topology and temperature.

Studies strongly indicate that CNTs (carbon nano tubes) play a critical role in the splat distribution and improvement [2]. Balani research group has worked extensively on the synthesis of CNT reinforced aluminum oxide coatings by plasma spray technique [3-5]. Balani

et al. obtained ~200% improvement in the elastic modulus, 57% improvement in the fracture toughness and 49 times enhancement in dry sliding wear resistance by adding 8 wt.% CNTs in Al<sub>2</sub>O<sub>3</sub> coatings[3-5].

Hence, study of splat distribution is extremely important for understanding micro sprayed coatings that reinforced with CNT. Development of splat distribution analyzes, which can predict morphology of splats, can potentially reduce the cost of the development of new coatings considerably.

Ideally, this distribution analyzes and models will allow us to adapt plasma-coating properties to meet the requirements of individual applications, without having to do extensive experimentation. The analysis will also enable us to predict, improve and optimize the design of existing spraying guns.

Droplets impact and splat formation in plasma spray researches can be broadly classified into one of two studies: morphology of splats or simulation of impact.

Many studies have been reported on the morphological aspect of splats which suggest that splat morphology is largely dependent on (i) feedstock material properties, (ii) thermal and



kinetic state of the in-flight particle and (iii) substrate chemical state, roughness and temperature [6, 7].

Elsebaei et al. presented a study on the morphology of individual splats for different sets of plasma operating parameters for the regular yttria stabilized zirconia (YSZ) (particle size: 45–100  $\mu\text{m}$ ) and the spherical agglomerate of YSZ (agglomerate size: 20–40  $\mu\text{m}$ ) synthesized from the nano-YSZ powder particle [7]. Lima et al. studied thermal spray coatings synthesized from the nanostructured ceramic agglomerated powder and concluded that it was necessary to avoid the full melting of the agglomerates to preserve nanostructure in the coating [8].

There exists a considerable literature describing simulation of droplet impact and splat spreading on a solid surface. Harlow and Shannon [9] were the first to simulate this phenomenon. They used a “marker-and-cell” (MAC) finite-difference method to solve the fluid mass and momentum conservation equations, while neglecting the effect of viscosity and surface tension to simplify the problem. Trapaga and Szekely [10] applied a commercial code, FLOW-3D [11], that uses the Volume-of-Fluid (VOF) method, to study impact of molten particles. Liu et al. [12] employed another VOF based code, RIPPLE [13], to simulate molten metal droplet impact. Bussmann et al. published a description of a three dimensional, finite-volume, fixed-grid Eulerian model they developed, which used a volume-tracking algorithm to locate the droplet free surface during its impact on a solid surface [14]. Pasandideh-Fard et al. [15] studied the three-dimensional model of Bussmann et al. [14] to include heat transfer and solidification. Asadi et al. extended numerical and analytical model of the inclined impact of a droplet on a solid surface in a thermal spray coating process [16]. Sedighi et al. studied the process of a single nanodroplet impact onto a surface with a molecular dynamics simulation (MD) using the interactions between molecules were represented by the Lennard-Jones (LJ) potential. They found that the dynamic contact angle and spreading diameter, as well as the advancing and receding time periods, exhibit strong dependence on droplet size [1, 17]. Asadi

et al. published a effect of contact angle on droplet impact onto a solid surface. He uses a molecular-kinetic theory in modeling contact angle to prevent the spreading-and-recoiling oscillations. Asadi [18] applied a modified computational fluid dynamics and molecular kinetic theory (CFD-MK) method to model the impact of nano droplets on the flat surface. He extended the model to include molecular kinetic theory and simulated impact of nano droplets falling on a flat plate.

However, in all previous studies the main attention has been focused on the splat morphology or simulation of splat formation. A literature survey carried out by the author indicated lack of published data on the CNT splat distribution analyzing by statistical distributions.

In the present work, we analyze the data of splats with carbon nanotube (CNT) addition, obtained in Keshri and Agarwal literature [2]. Such a selection of splat dataset will allow us to statistically analyze the spread property of a range of materials i.e. sub-micron  $\text{Al}_2\text{O}_3$  powder was spray dried (referred as A-SD) to sub-micron  $\text{Al}_2\text{O}_3$  with 4 wt.% CNTs (referred as A4C-SD) and 8 wt.% CNTs (referred as A8C-SD) materials. For this purpose, we study the spreading data using different distribution functions. It is observed that the spreading data is always positive and therefore, it is reasonable to analyze of this data using the probability distribution, which has support only on the positive real axis. Thus, we have considered different two-parameter distributions namely, generalized exponential, Burr X, Weibull and Burr III distributions. For choosing the best fitted model to a given datasets, we use different criteria such as AIC, BIC, LL and K-S distance. For computing the different criteria, we estimate the unknown parameters using the Maximum Likelihood (ML) method. The rest of the paper is organized as follows. In Section 2, we describe the different probability models. The model selection criteria are provided in Section 3. Results of spread data are provided in Section 4. Finally we conclude the paper in section 5.

## 2. DIFFERENT PROBABILITIES MODELS

### 2. 1. Generalized Exponential Distribution

The two-parameter generalized exponential (GE) distribution has been studied extensively by Gupta and Kundu [19]. The two-parameter GE distribution has the following density function

$$f(x; \alpha, \beta) = \alpha\beta e^{-\beta x} (1 - e^{-\beta x})^{\alpha-1} \quad \alpha, \beta > 0 \quad (1)$$

Here  $\alpha$  and  $\beta$  are the shape and scale parameters respectively. Therefore, the maximum likelihood estimators (MLEs) of  $\alpha$  and  $\beta$  can be obtained by maximizing the following log-likelihood function with respect to the unknown parameters;

$$L_{GE}(\alpha, \beta | data) = n \ln(\alpha) + n \ln(\beta) -$$

$$\beta \sum_{i=1}^n \ln(x_i) + (\alpha - 1) \sum_{i=1}^n \ln(1 - e^{-\beta x_i}) \quad (2)$$

The MLEs of  $\alpha$  and  $\beta$ , say  $\hat{\alpha}$  and  $\hat{\beta}$  respectively can be obtained as the solutions of

$$\frac{\partial L}{\partial \alpha} = \frac{n}{\alpha} + \sum_{i=1}^n \ln(1 - e^{-\beta x_i}) = 0 \quad (3)$$

$$\frac{\partial L}{\partial \beta} = \frac{n}{\beta} - \sum_{i=1}^n \ln x_i + (\alpha - 1) \sum_{i=1}^n \frac{x_i e^{-\beta x_i}}{1 - e^{-\beta x_i}} = 0 \quad (4)$$

From (3), we have

$$\hat{\alpha} = - \frac{n}{\sum_{i=1}^n \ln(1 - e^{-\hat{\beta} x_i})} \quad (5)$$

Substituting  $\hat{\alpha}$  in (2), we obtain the profile log-likelihood of  $\beta$  as

$$g(\beta) = L(\hat{\alpha}, \beta) = -n \ln \left( \sum_{i=1}^n \ln(1 - e^{-\beta x_i}) \right) + n \ln \beta - \beta \sum_{i=1}^n x_i - \sum_{i=1}^n \ln(1 - e^{-\beta x_i}) \quad (6)$$

Therefore, the MLE of  $\beta$ , can be obtained by maximizing (6) with respect to  $\beta$ . It is clear that the maximum of (6) can be obtained as a fixed point solution of the following equation;

$$u(\beta) = \beta \quad (7)$$

Where

$$u(\beta) = n \left[ \frac{n}{\sum_{i=1}^n \ln(1 - e^{-\beta x_i})} \left( \sum_{i=1}^n \frac{x_i e^{-\beta x_i}}{1 - e^{-\beta x_i}} \right) + \sum_{i=1}^n \frac{x_i}{1 - e^{-\beta x_i}} \right]^{-1}$$

The solution of (7) can be obtained by a very simple iterative procedure. Suppose we start with an initial guess  $\beta_{(0)}$  then the next iterate  $\beta_{(1)}$  can be obtained as  $\beta_{(1)} = u(\beta_{(0)})$ , similarly,  $\beta_{(2)} = u(\beta_{(1)})$  and so on. Finally, the iterative procedure should be stopped when  $|\beta_{(i+1)} - \beta_{(i)}| < \epsilon$ . Once we get the MLE of  $\beta$  the MLE of  $\alpha$  can be obtained from (5).

### 2. 2. Burr Type X Distribution

The Burr Type X (BX) distribution due to Burr [20] has the probability density function (pdf) for  $x > 0$  as

$$f(x; \alpha, \beta) = 2\alpha\beta^2 x e^{-(\beta x)^2} (1 - e^{-(\beta x)^2})^{\alpha-1} \quad \alpha, \beta > 0$$

Here also  $\alpha$  and  $\beta$  are the shape and scale parameters respectively. The maximum likelihood estimators of  $\alpha$  and  $\beta$  can be obtained by maximizing the log-likelihood function

$$L_{BX}(\alpha, \beta | data) \propto n \ln(\alpha) + 2n \ln(\beta) + \sum_{i=1}^n \ln(x_i) - \beta^2 \sum_{i=1}^n x_i^2 + (\alpha - 1) \sum_{i=1}^n \ln(1 - e^{-(\beta x_i)^2})$$

with respect to the  $\alpha$  and  $\beta$ . So, if  $\hat{\alpha}$  and  $\hat{\beta}$  are the maximum likelihood estimators of  $\alpha$  and  $\beta$  respectively, then

$$\hat{\alpha} = - \frac{n}{\sum_{i=1}^n \ln(1 - e^{-(\hat{\beta} x_i)^2})}$$

Similarly, the maximum likelihood estimator of  $\beta$  can be obtained by maximizing the following profile log-likelihood function as:



$$g(\beta) = L(\hat{\alpha}, \beta) = n \ln \left( - \sum_{i=1}^n \ln(1 - e^{-(\beta x_i)^2}) \right) + 2n \ln \beta - \beta^2 \sum_{i=1}^n x_i^2 - \sum_{i=1}^n \ln(1 - e^{-(\beta x_i)^2})$$

### 2. 3. Weibull Distribution

The two-parameter Weibull (W) distribution for  $x > 0$  has the following density function;

$$f(x; \alpha, \beta) = \alpha \beta x^{\alpha-1} e^{-\beta x^\alpha} \quad \alpha > 0, \beta > 0$$

Here  $\alpha$  and  $\beta$  represent the shape and scale parameters respectively. The maximum likelihood estimators of  $\alpha$  and  $\beta$  can be obtained by maximizing the log-likelihood function

$$L_w(\alpha, \beta | data) = n \ln \alpha + n \ln \beta - \beta \sum_{i=1}^n x_i^\alpha + (\alpha - 1) \sum_{i=1}^n \ln x_i$$

with respect to the unknown parameters. Therefore, if  $\hat{\alpha}$  and  $\hat{\beta}$  are the maximum likelihood estimators of  $\alpha$  and  $\beta$  respectively, then

$$\hat{\beta} = \frac{n}{\sum_{i=1}^n x_i^\alpha}$$

Furthermore, the maximum likelihood estimator of  $\alpha$  can be obtained by maximizing the profile log-likelihood of  $\alpha$  as  $g(\alpha) = L(\alpha, \hat{\beta})$ .

### 2. 4. Burr Type III Distribution

The Burr Type III (BIII) distribution also due to Burr [20] is given by the pdf

$$f(x, \alpha, \beta) = \alpha \beta x^{-\beta-1} (1 + x^{-\beta})^{-(\alpha+1)} \quad \alpha, \beta > 0$$

Here  $\alpha$  and  $\beta$  are two shape parameters. The maximum likelihood estimator of  $\alpha$  and  $\beta$  say  $\hat{\alpha}$  and  $\hat{\beta}$  can be obtained similarly.

## 3. MODEL SELECTION CRITERIA

It may be of interest for a given data to determine which of the above mentioned distributions provides the best fit. Therefore, in this section, we provide different criteria for

selecting the best fitted distribution of these datasets.

### 3. 1. Kolmogorov- Smirnov Distance

The Kolmogorov distance is one of important distances between two distribution functions, say  $F$  and  $G$  and has been used in many problems and it can be described as follows;

$$D(F, G) = \sup_{-\infty < x < \infty} |F(x) - G(x)|$$

To implement this procedure, a candidate from each parametric family that has the smallest Kolmogorov distance should be found and then the different best fitted distributions should be compared.

### 3. 2. Akaike's Information Criterion

Consider a sample of independently identically distributed (*i.i.d.*) random variables,  $X_1, \dots, X_n$  having probability density function  $h(x) = h$ . Let us consider two rival models:

$$F^\alpha = \{f^\alpha(\cdot), \alpha \in M \subseteq R^p\} = (f) \text{ and}$$

$$G^\beta = \{g^\beta(\cdot), \beta \in B \subseteq R^q\} = (g).$$

The KL information in favor of  $h$  against  $f^{\hat{\alpha}}$  is defined as

$$KL(h, f^\alpha) = E_h \left( \log \frac{h(X)}{f^\alpha(X)} \right) = \int_{-\infty}^{\infty} h(x) \log \frac{h(x)}{f^\alpha(x)} dx$$

We have  $KL(h, f^\alpha) \geq 0$  and  $KL(h, f^\alpha) = 0$ , imply that  $h = f^\alpha$ , that is  $\alpha = \alpha_0$ . The KL divergence is often intuitively interpreted as a distance between the two probability measures, but this is not mathematically a distance; in particular, the KL divergence is not symmetric. The Akaike [21] introduced the Akaike information criterion (AIC) to select the best model under parsimony. The goal of AIC is to minimize the KL divergence of the selected model from the true model. Notice that the important part of the KL

divergence is  $E_k(\log f^\alpha(X))$  which has an estimator as

$$\frac{1}{n} \sum_{i=1}^n \log f^{\hat{\alpha}_n}(x_i)$$

It can be considered as an estimator of the divergence between the true density and the model. Akaike introduced his criterion to model selection as

$$AIC^f = -2 \sum_{i=1}^n \log f^{\hat{\alpha}_n}(x_i) + 2p$$

Where,  $p$  is the number of parameters in the model. Now between the two families  $F$  and  $G$  choose family  $F$  if  $AIC^f < AIC^g$  and choose family  $G$  otherwise.

### 3. 3. Bayesian Information Criterion

The Bayesian information criterion (BIC) is one of the important criteria for determining the best model for a given data. One major difference of this criterion is the different penalty term that it uses. Thus BIC [22] is defined as

$$BIC^f = -2 \sum_{i=1}^n \log f^{\hat{\alpha}_n}(x_i) + p \log n$$

The BIC is based on Bayesian probability and can be applied to models estimated by the maximum

likelihood method and the most well-known properties of BIC is asymptotic (loss) optimality and consistency (in selection), respectively. So, we choose family  $F$  if  $BIC^f < BIC^g$ ; otherwise we choose family  $G$ .

### 3. 4. Maximum Likelihood Criterion

Cox's test [23] as a modified log-likelihood ratio statistic involves centering the log-likelihood ratio statistic under the null hypothesis. Cox's statistic is given by

$$C(\hat{\alpha}_n, \hat{\beta}_n) = \sum_{i=1}^n \left\{ \ln(f^{\hat{\alpha}_n}(x_i)) - \ln(g^{\hat{\beta}_n}(x_i)) \right\}$$

Here,  $\hat{\alpha}_n$  and  $\hat{\beta}_n$  are maximum likelihood estimators of  $\alpha$  and  $\beta$  respectively. Choose the family  $F$  if  $C > 0$ , otherwise choose  $G$ . It is known that normalized of  $c(\hat{\alpha}_n, \hat{\beta}_n)$  has asymptotically standard normal distribution [24].

## 4. RESULTS

For A-SD, A4C-SD and A8C-SD splat datasets (see, Ref.[2]), first we presented the descriptive statistics for three datasets in Table 1. It is observed that the highest mean value is in A8C-SD with a standard deviation of 1.3046. Also, we have fitted different distributions and the estimated parameter values, AIC values, BIC

Table 1. Descriptive statistics of spread datasets.

Dataset	n	Mean	SD	Min	Max
A-SD	90	28.65	1.4537	26.25	31.75
A4C-SD	92	34.75	1.4741	32.25	37.75
A8C-SD	92	43.28	1.3046	40.25	46.25

Table 2. Estimated parameters, K-S distances and AIC values for different distribution functions of A-SD.

Distribution	Estimated parameters		K-S	AIC	BIC	LL
GE	$\alpha = 3.775 \times 10^8$	$\beta = 0.7061$	0.1005	$3.290 \times 10^2$	$3.340 \times 10^2$	$-1.625 \times 10^2$
BX	$\alpha = 5.1509 \times 10^4$	$\beta = 0.11781$	0.1320	$4.509 \times 10^2$	$4.559 \times 10^2$	$-3.328 \times 10^2$
BIII	$\alpha = 9.908 \times 10^9$	$\beta = 6.8978$	0.3622	$4.510 \times 10^2$	$4.560 \times 10^2$	$-2.235 \times 10^2$
W	$\alpha = 5.383 \times 10^4$	$\beta = 2.2335$	0.5486	$6.442 \times 10^2$	$6.492 \times 10^2$	$-3.201 \times 10^2$



**Table 3.** Estimated parameters, K-S distances and AIC values for different distribution functions of A4C-SD.

Distribution	Estimated parameters		K-S	AIC	BIC	LL
GE	$\alpha = 3.398 \times 10^9$	$\beta = 0.6435$	0.1125	$3.422 \times 10^2$	$3.472 \times 10^2$	$-1.691 \times 10^2$
BX	$\alpha = 3.274 \times 10^5$	$\beta = 0.1045$	0.1134	$4.639 \times 10^2$	$4.690 \times 10^2$	$-3.486 \times 10^2$
BIII	$\alpha = 1.036 \times 10^{10}$	$\beta = 6.54449$	0.4070	$5.032 \times 10^2$	$5.081 \times 10^2$	$-2.495 \times 10^2$
W	$\alpha = 6.163 \times 10^4$	$\beta = 2.09692$	0.5925	$7.054 \times 10^2$	$7.105 \times 10^2$	$-3.507 \times 10^2$

**Table 4.** Estimated parameters, K-S distances and AIC values for different distribution functions of A8C-SD.

Distribution	Estimated parameters		K-S	AIC	BIC	LL
GE	$\alpha = 1.124 \times 10^9$	$\beta = 0.4883$	0.1285	$3.580 \times 10^2$	$3.631 \times 10^2$	$-1.770 \times 10^2$
BX	$\alpha = 5.2167 \times 10^6$	$\beta = 0.0921$	0.1295	$4.545 \times 10^2$	$4.596 \times 10^2$	$-3.525 \times 10^2$
BIII	$\alpha = 1.319 \times 10^7$	$\beta = 4.3961$	0.4737	$6.125 \times 10^2$	$6.175 \times 10^2$	$-3.042 \times 10^2$
W	$\alpha = 1.934 \times 10^{-1}$	$\beta = 0.4094$	0.5845	$10.463 \times 10^2$	$10.514 \times 10^2$	$-5.212 \times 10^2$

values, K-S distances and the log-likelihood (LL) values are reported in Tables 2, 3 and 4 respectively. From Tables 2, 3 and 4, it is clear that, GE is the best fitted model based on the maximum log-likelihood values, minimum AIC and BIC values or the minimum Kolmogorov distance. We also plot the fitted probability distribution function and the relative histogram for different distributions and for all datasets in

Figures 1, 2 and 3 respectively. For more comparison purposes we present the q-q plots of GE distribution for datasets 1, 2 and 3 in Figures 4-6 respectively. These plots show a strong relationship supporting the appropriateness of the GE distribution. For all datasets, it can be noted that that shape parameter of the GE distribution is very high. It shows that the mean, median and mode are approximately equal to  $\log \alpha$ .

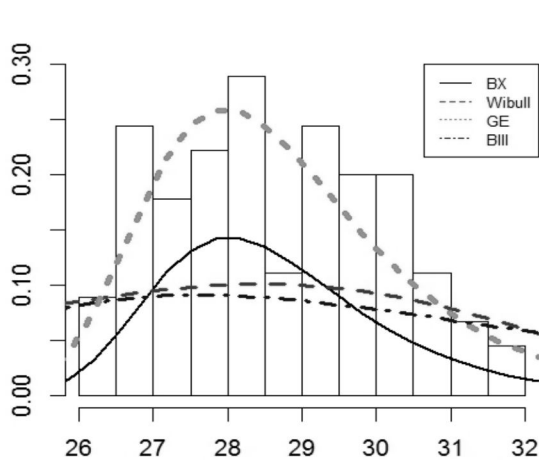


**Fig. 1.** The fitted probability distribution function (pdf) and the relative histogram for A-SD data.

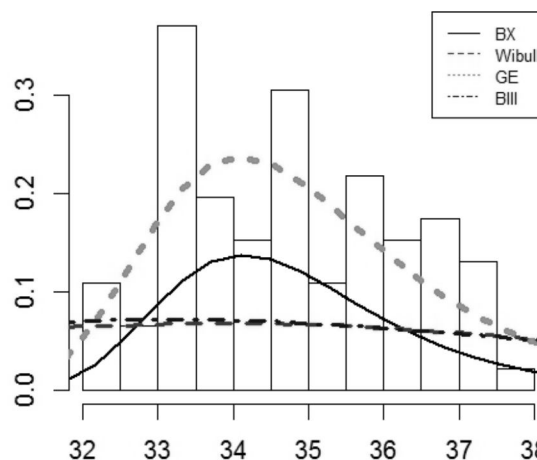


**Fig. 2.** The fitted probability distribution function (pdf) and the relative histogram for A4C-SD data.

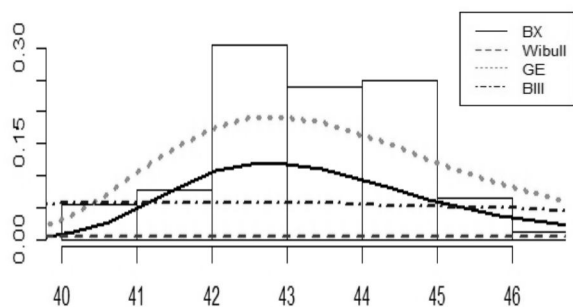


Fig. 3. The fitted probability distribution function (pdf) and the relative histogram for A8C-SD data.

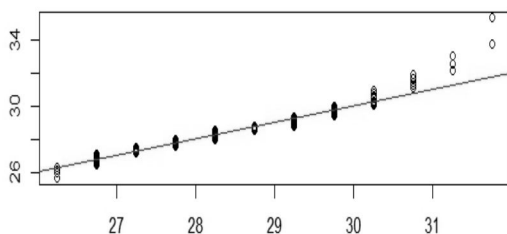


Fig. 4. The q-q plot of A-SD data.

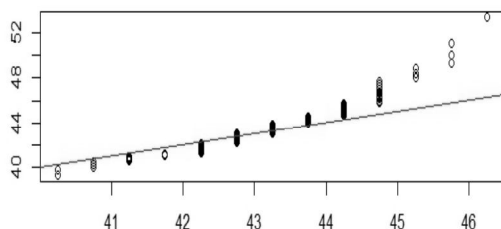


Fig. 5. The q-q plot of A4C-SD data.

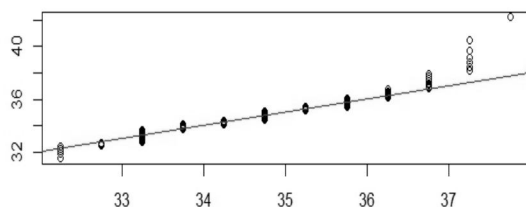


Fig. 6. The q-q plot of A8C-SD data

## 5. CONCLUSIONS

In order to describe the behavior of the spread data of aluminum oxide splats reinforced with carbon nanotubes., it is required to identify the distribution, which best fit the data. So, the aim of this paper is to compare different probability models namely, Weibull, Burr X, generalized exponential and Burr III for these datasets. Different plots and statistical criteria were used to identify the best fitted distribution for these datasets. Using several statistical criteria, like minimum Kolmogorov distance, minimum AIC values, minimum BIC values and maximum log-likelihood value, the GE distribution function appears to be more appropriate statistical distribution function in these datasets. The result of our study is important in coating industries and that is the droplet spread of spray coatings should be described using several statistical criteria and different distribution functions, as studied in the present paper.

## ACKNOWLEDGEMENTS

The author would like to thank Dr. H. Panahi (faculty member of statistical department of Lahijan Azad University) for many stimulating discussions. This research was supported in part from a grant (no. 0107/7/111) from the Research Deputy of Payame Noor University. Their support is gratefully acknowledged.

## REFERENCES

1. Sedighi, N. Murad, S. and Aggarwal, S., K., Molecular dynamics simulations of spontaneous spreading of a nanodroplet on solid surfaces. *fluid dynamics research*, 2011, 43, 1-23.
2. Keshri, A. K. and Agarwal, A., Splat morphology of plasma sprayed aluminum oxide reinforced with carbon. *Surf. Coat. Technol.*, 2011, 206, 338-347.
3. Balani, K. and Agarwal, A., Wetting of carbon nanotubes by aluminum oxide. *Nanotechnology*, 2008, 19, 16, 165-172.
4. Balani, K. and Agarwal, A., Damping behavior of carbon nanotube reinforced aluminum oxide coatings by nanomechanical dynamic modulus



- mapping. *J. Appl. Phys.*, 2008, 104, 6.
5. Balani, K. and Agarwal, A., Process map for plasma sprayed aluminum oxide-carbon nanotube nanocomposite coatings. *Surface & Coatings Technology*, 2008, 202, 17, 4270-4277.
  6. Sampath, S. and Jiang, X., Splat formation and microstructure development during plasma spraying: deposition temperature effects. *Materials Science and Engineering*, 2001, 304-306, 144-150.
  7. Elsebaei, A., et al., Comparison of In-Flight Particle Properties, Splat Formation, and Coating Microstructure for Regular and Nano-YSZ Powders. *J. Therm. Spray Technol.*, 2010, 19, 2-10.
  8. Lima, R. S. and Marple, B. R., Thermal Spray Coatings Engineered from Nanostructured Ceramic Agglomerated Powders for Structural, Thermal Barrier and Biomedical Applications: A Review. *J. Therm. Spray Technol.*, 2007, 16, 1, 40-63.
  9. Harlow, F. H. and Shannon, J. P., The splash of a liquid droplet. *J. Appl. Phys.*, 1967, 38.
  10. Trapaga, G. and Szekely, J., Mathematical modeling of the isothermal impingement of liquid droplets in spraying processes. *Metall. Trans. B*, 1991, 22.
  11. FLOW-3D: computational modelling power for scientists and engineers. 1988: Flow Science Inc., San Diego, CA.
  12. Liu, H.; Lavernia, E. J. and Rangel, R. H., Numerical simulation of substrate impact and freezing of droplets in plasma spray processes. *Journal of Physics: D Applied Physics*, 1993, 26, 1900-1908.
  13. Kothe, D. B.; Mjolsness, R. C. and Torrey, M. D., RIPPLE: a computer program for incompressible flows with free surfaces. 1991: LANL, Los Alamos, NM, .
  14. Bussmann, M.; Mostaghimi, J. and Chandra, S., On a three-dimensional volume tracking model of droplet impact. *Phys. Fluids*, 1999, 11, 1406-1417.
  15. Pasandideh-Fard, M.; Chandra, S. and Mostaghimi, J., A three-dimensional model of droplet impact and solidification. *International Journal of Heat & Mass Transfer*, 2002, 45, 10, 2229-2242.
  16. Asadi, S.; Passandideh-Fard, M. and Moghiman, M., Numerical and analytical model of the inclined impact of a droplet on a solid surface in a thermal spray coating process. *Iran. J. Surf. Eng.*, 2008, 4, 1-14.
  17. Sedighi, N.; Murad, S. and Aggarwal, S. K., Molecular dynamics simulations of nanodroplet spreading on solid surfaces, effect of droplet size. *Fluid Dynamics Research*, 2010, 42, 3.
  18. Asadi, S., Simulation of nanodroplet impact on a solid surface. *Inter. J. Nano Dim.*, 2012, 3, 1, 19-26.
  19. Gupta, R. and Kundu, D., Generalized exponential distributions; statistical inferences. *Journal of Statistical Theory and Applications*, 2002, 1, 1, 101-118.
  20. Burr, I. W., Cumulative frequency distribution. *Annals of Mathematical Statistics*, 1942, 13, 215-232.
  21. Akaike, H. Information theory and an extension of the maximum likelihood principle. in *Second international symposium on information theory*. 1973. Akademinai Kiado.
  22. Schwarz, G., Estimating the dimension of a model. *The annals of statistics*, 1978, 6, 2, 461-464.
  23. Cox, D. R., Further results on tests of separate families of hypotheses. *Journal of the Royal Statistical Society. Series B (Methodological)*, 1962, 406-424.
  24. White, H., Regularity conditions for Cox's test of non-nested hypotheses. *Journal of Econometrics*, 1982, 19, 2, 301-318.